Chemical Engineering Journal Advances 27 (2026) 101221

Contents lists available at ScienceDirect

Chemical Engineering Journal Advances

journal homepage: www.sciencedirect.com/journal/chemical-engineering-journal-advances

Methanation of metal carbonates with mechano-energy using H_2O as a reducing agent

Naoya Ito [a,b], Naoya Sakurada [a], Tatsunori Iwamura [a,b], Takashi Ikawa [a,*], Hironao Sajiki [a,b,*]

[a] Laboratory of Advanced Chemistry and Next Generation Energy Chemistry Joint Research Laboratory, Gifu Pharmaceutical University, Daigaku-Nishi, Gifu 501-1196, Japan
[b] Department of Applied Chemistry, Faculty of Engineering, Aichi Institute of Technology, 1247 Yachigusa, Yakusa-cho, Toyota 470-0392, Japan

ARTICLE INFO

Keywords:
Metal carbonates methanation
Mechanochemical reaction
Nickel/Aluminum alloy
H_2O as a reducing agent

ABSTRACT

Development of methanation processes from metal carbonates is important for carbon-neutral energy systems, however, the high chemical stability of carbonates limits direct conversion to methane. Here, we report a mechanochemical approach for methane production from metal carbonates. Using a commercially available Ni/Al alloy and H_2O, methane formation from relatively unreactive carbonates proceeded without external heating or hydrogen pressurization. Under the conditions, high yields of methane (up to > 99%) were obtained from several carbonates, especially calcium carbonate, manganese carbonate hydrate, and copper carbonate -copper hydroxide complex. X-ray photoelectron spectroscopy (XPS) analysis of the Ni/Al powder at different reaction stages suggested a reversible change in the nickel oxidation state [Ni (0) → Ni (II) → Ni (0)] during the process. The present method enables methane production under mild conditions and shows potential for improved energy efficiency compared with previously reported approaches.

1. Introduction

Reducing carbon dioxide (CO_2) emissions, a major greenhouse gas that contributes to global warming, is a global challenge to meeting the goals of the Glasgow Climate Pact [1–9]. The overarching objective of the Accord is to restrict the increase in global temperature since the pre-industrial era to 1.5 °C. While the transition to low-carbon energy resources and improved energy efficiency are of paramount importance, achieving these goals without compromising industrial and economic stability requires more than just emission reduction. It also calls for technologies such as Carbon Dioxide Capture and Storage (CCS), which involves the separation, capture, and subsurface storage of CO_2, and Carbon Dioxide Capture and Utilization (CCU), which includes the separation and capture of CO_2 followed by its subsequent utilization. However, the potential of CCU is limited to applications such as dry ice, concrete materials, polycarbonate, or the fixation of organic compounds. One of the most significant and viable strategies to combat global warming is the conversion of CO_2 into synthetic methane (CH_4), followed by its use as a fuel in a carbon-neutral cycle. This approach serves as a direct alternative to fossil fuels. However, realizing this goal requires not only reducing energy input and costs associated with CO_2 capture and purification, but also ensuring that the overall costs and infrastructure required for the catalytic conversion of CO_2 into methane are more competitive than those for natural gas.

Ball milling is a versatile and environmentally friendly technique that provides a robust foundation for advancing novel synthetic methodologies, aligning with the principles of green chemistry. Considering this, the present study has investigated the potential of ball-mill-mediated mechanochemical reactions across a broad range of organic transformations. The pursuit of carbon neutrality has resulted in a notable emphasis on CO_2 capture, utilization and storage (CCUS) technologies. A plethora of CO_2-to-methane conversion methods have been developed and documented in review papers [10–20]. CO_2 capture from industrial exhaust gases is a pivotal component of the CCUS technology. A simple method for capturing CO_2 involves the use of alkaline water, where the conversion of CO_2 into carbonate enhances CCUS processes by enabling CO_2 storage at elevated concentrations. Calcium carbonate ($CaCO_3$), the most abundant carbonate in Earth's crust and in stalactites, is mainly responsible for the long-term fixation of CO_2 on Earth. Therefore, developing an effective method to convert $CaCO_3$ to CH_4

* Corresponding authors.
E-mail addresses: ikawa-ta@gifu-pu.ac.jp (T. Ikawa), sajiki@gifu-pu.ac.jp, sajikih@aitech.ac.jp (H. Sajiki).

https://doi.org/10.1016/j.ceja.2026.101221

Available online 9 May 2026

could provide a net-zero-emission fuel. Developing this ideal fuel is feasible without releasing more CO_2 than was originally captured from the atmosphere, thereby establishing and maintaining a sustainable CO_2 cycle. The present study has established a method for the conversion of $CaCO_3$ into CH_4. However, conventional methods for converting chemically stable carbonates into CH_4, including the decomposition of solid metal carbonates, typically require elevated temperatures and pressurized hydrogen (H_2) [21–27]. Considerable research has focused on catalysts in the hydrogenation of carbonates to reduce hydrogen pressure and reaction temperature. As stated by Padeste *et al.* [21], the conversion of $CaCO_3$ to methane and CO_2 can be achieved at temperatures ranging from 527 to 700 °C and H_2 pressures between 0.1 and 6.0 MPa. Tsuneto *et al.* (1992) [22] reported that $CaCO_3$ mixed with 2 wt% cobalt (Co) and nickel (Ni) powder was converted to a small amount of methane at 400 °C under a H_2 atmosphere for 1 h. Yoshida *et al.* (1999) [23] reported that the catalytic hydrogenation of $CaCO_3$ occurs at approximately 300 °C under a H_2 atmosphere using palladium (Pd) and iridium (Ir) powder as catalysts to produce methane. Mesters *et al.* [24] demonstrated that magnesium carbonate ($MgCO_3$) can undergo direct hydrogenation to methane using a commercially available nickel catalyst (KL6516-CY1.2). In continuous-flow and batch reactor experiments, high Ni/$MgCO_3$ ratios (9:1 w/w) at 350–360 °C resulted in the methanation of $MgCO_3$, yielding methane at 17% yield, while no CO was detected under these conditions. Shen *et al.* [25] reported that the in-situ Ni catalyst, generated from $NiCO_3$, was utilized for the hydrogenation of $CaCO_3$ to methane at an elevated temperature of 400 °C. This reaction was facilitated by 9,10-dihydrophenanthrene (DHP), which acted as a liquid organic H_2 carrier. The process yielded methane with a 40% yield and approximately 90% selectivity. Similarly, Shi *et al.* [26] reported that the in-situ production of Ni from $NiCO_3$ promoted the conversion of $CaCO_3$ to methane, achieving nearly quantitative methane conversion at 508 °C under H_2 atmosphere.

In this study, we investigated the mechanochemical conversion of carbonate compounds to methane using Ni/Al alloy under solvent-free ball-milling conditions. The effects of the amount of Ni/Al alloy and carbonate species on the formation of CH_4, H_2, and CO_2 were systematically evaluated. Furthermore, the surface chemical states of the reacted samples were analyzed by X-ray photoelectron spectroscopy (XPS) to examine changes in the Ni and Al species during the reaction. These results elucidate the relationship between reaction conditions and gas product distributions, and provide fundamental insights into mechanochemical carbonate methanation using Ni/Al alloy.

2. Materials and methods

2.1. General experimental procedure for mechanochemical carbonate methanation

A carbonate (3.1 mmol), distilled H_2O (270 μL, 15 mmol), and SUS304 balls (ca. 5 mm diameter, 100 pieces) were placed in an 80 mL SUS440C vessel, and tightly sealed with a designated SUS440C lid. The vessel was rotated using a planetary ball mill (Fritsch Pulverisette Premium Line 7 [PLP-7]) ball mill) at a rotating speed of 1,100 rpm for 90 min. The rotation was split into three 30 min segments for 1 min interval, and the rotation was turned over alternately every 30 min (inverse rotation).

After the reaction, the tightly enclosed vessel was placed in a water bath and opened. The resulting gas was collected over water with a measuring cylinder, then transferred into an aluminum gas collecting bag by the downward displacement of water. The gas composition was determined by gas chromatography equipped with a thermal conductivity detector (GC-TCD, GC-3200, GL Sciences Inc.). Unless otherwise indicated, all experiments were conducted under the after-mentioned conditions.

Unless otherwise noted, all reactions were carried out under identical conditions. Detailed experimental procedures, including milling conditions, gas collection methods, and analytical protocols, are described in the Supplementary Information.

2.2. Carbonates

The following carbonates were used without further purification: Na_2CO_3, K_2CO_3, $MgCO_3$, $CaCO_3$, $BaCO_3$, $MnCO_3{\cdot}nH_2O$, $FeCO_3$, $NiCO_3$, $CuCO_3{\cdot}Cu(OH)_2$, and $ZnCO_3{\cdot}Zn(OH)_2$. The sources and purities of these materials are provided in the Supplementary Information.

2.3. The effect of Ni-based additives

The reactions were carried out according to the general procedure described in Section 2.1, using $CaCO_3$ as the substrate and various Ni-based additives (1.0 equivalent). The additives included Ni/Al alloy, Ni powder, $Ni(OH)_2$, $Ni(OAc)_2{\cdot}4H_2O$, NiO, and Raney Ni.

2.4. Effect of additives

The reactions were performed following the general procedure (Section 2.1), with the addition of various additives (1.0 equivalent). These included Al metal powder and Al_2O_3.

Unless otherwise noted, stainless-steel milling media were used. Control experiments employing zirconia (ZrO_2) vessels and balls were conducted to exclude the contribution of metallic components. Experimental details are described in the Supplementary Information.

2.5. Gas analysis

The yields of CH_4, H_2, and CO_2 (%) were calculated based on the initial amount of carbonate or H_2O. The CH_4 yield was defined on a carbon basis relative to the initial carbonate. The H_2 yield (%) was defined as the molar ratio of generated H_2 to the theoretical maximum amount obtainable from the added H_2O, indicating the conversion efficiency of H_2O to H_2. The CO_2 yield was defined relative to the carbonate.

The conversion of H_2O was estimated from the total amount of hydrogen incorporated into gaseous products (H_2 and CH_4), assuming H_2O as the sole hydrogen source.

Detailed calculation methods, calibration procedures, and representative chromatograms are provided in the Supplementary Information.

Representative experiments were performed in triplicate to confirm reproducibility, and consistent trends were observed across all conditions.

2.6. Characterization

X-ray photoelectron spectroscopy (XPS), powder X-ray diffraction (XRD), and inductively coupled plasma (ICP) analyses were performed to characterize the reaction samples. Detailed experimental conditions and analytical procedures are provided in the Supplementary Information.

3. Results and discussion

In our previous study, we detailed a methodology for the mechanochemical reduction of gaseous CO_2 to CH_4 in a planetary ball mill. In the present study, the primary step involved the precise loading of solid metal carbonates (3.1 mmol) along with H_2O (270 μL, 15 mmol) into an 80 mL SUS440C vessel, which was hermetically sealed and operated under ambient conditions. This setup stimulated the mechanochemical conversion of gaseous CO_2 into CH_4 [28–31]. Subsequently, the mixture was subjected to rotation at 1,100 rpm using a planetary ball mill (PLP-7) with SUS304 balls (100 balls; each with diameter of approximately 5 mm). To prevent potential instrument failure, the rotation

direction of the planetary ball mill was reversed at 30 min intervals, with each reversal lasting 1 min. Mechanochemical generation of H_2 from H_2O was observed to occur to a modest or considerable extent in the presence of Na_2CO_3, K_2CO_3, $CaCO_3$, and $BaCO_3$. However, CH_4 generation was almost entirely absent (GC-TCD; Table 1, Entries 1, 2, 4, and 5) under these conditions. In contrast, no detectable generation of H_2 or conversion of carbonate to CH_4 was observed when $MgCO_3$, $MnCO_3$, $CuCO_3$, and $ZnCO_3$ were used (Entries 3, 6, 10, and 11). In case of $FeCO_3$, a slight generation of CH_4 and H_2 was observed (Entry 7). Further, in $NiCO_3$, a moderate conversion to CH_4 and quantitative H_2 generation were observed (Entry 8). The efficiency of $NiCO_3$ conversion to CH_4 was marginally enhanced by reducing the amount of H_2O added (Entry 9). The results indicated that the Ni cation was the key component of this reaction; the addition of 1.0 equivalent of Ni/Al alloy powder to the reaction mixture (Table 2, Entry 1) was found to be a key factor in the observed outcome. Moreover, $CaCO_3$ underwent quantitative conversion to CH_4, along with high-efficiency generation of H_2 (Table 2, Entry 1). However, the utilization of 1.0 equivalent of Ni powder or NiO only marginally enhanced the conversion efficiency of $CaCO_3$ to CH_4 and H_2 (Entries 2 and 5). The addition of 1.0 equivalent of $Ni(OH)_2$ or $Ni(OAc)_2{\cdot}4H_2O$ resulted in the conversion of $CaCO_3$ to CO_2, albeit with a moderate to low efficiency. However, the conversion of $CaCO_3$ to CH_4 and H_2 was not improved (Entries 3 and 4). It is noteworthy that the addition of 1.0 equivalent of Raney Ni— prepared via the activation of Ni/Al alloy using alkaline water, such as aqueous NaOH, to selectively elute the Al metal from the alloy—in place of Ni/Al alloy, had no effect on the conversion efficiency of $CaCO_3$ to CH_4 or H_2 generation (Entry 6). Therefore, it was confirmed that Al metal plays a pivotal role in the methanation reaction mediated by the Ni/Al alloy.

The substitution of 1.0 equivalent of Al or Al_2O_3 with a Ni/Al alloy resulted in increased H_2 generation. However, the conversion efficiency of $CaCO_3$ exhibited only a slight improvement and was not enhanced by the addition of either Ni powder (Table 2, Entry 2) or Al powder (Table 3, Entry 1). However, when a combination of Ni powder (1.0 equivalent) and Al powder (1.0 equivalent) was used, the conversion efficiency of $CaCO_3$ to CH_4 was enhanced to 18%, accompanied by the H_2 generation in an efficient manner (71%, Entry 3). Furthermore, the combination of Ni powder and Al_2O_3, used as the substitutes for Ni/Al alloy, enhanced the conversion efficiency of $CaCO_3$ to CH_4 to 24%, and the H_2 generation to 78% (Entry 4). Quantitative conversion of $CaCO_3$ to CH_4 was observed when Ni and Al powders were used in a 2: 1 molar ratio (Al: Ni), corresponding to the metal composition of the Ni/Al alloy (with a Ni: Al weight ratio of 1: 1). However, the H_2 generation decreased to 39%, equivalent to approximately 6 mmol. Experimental data show that 15 mmol of water is utilized, indicating that about 9 mmol of hydrogen is consumed in the reduction of $CaCO_3$. This observation is consistent with the anticipated outcome of converting CO_2 to CH_4, and H_2O, as documented in Entry 5. A decrease in the amount of Ni/Al alloy powder from 1.0 equivalent to 0.05 equivalents led to a marked reduction in the conversion efficiency of $CaCO_3$ to CH_4 and in H_2 generation, as shown in Table 4, Entry 1. This discrepancy is attributed to the requirement for sufficient active metal surface sites under mechanochemical conditions. When a stoichiometric amount of Ni/Al alloy is used, efficient contact between the reactants and the catalytic surface is achieved, resulting in high CH_4 formation. In contrast, a reduced amount of Ni/Al alloy results in insufficient contact between reactants and the catalytic surface, significantly decreasing the reaction efficiency. On the other hand, increasing the amount of Ni/Al alloy had no effect on the conversion efficiency of $CaCO_3$, regardless of the quantity used (i.e. 0.05 equivalents, 0.10 equivalents, 0.30 equivalents, and 0.50 equivalents). However, a slight enhancement in H_2 generation was observed in Entries 2, 3, and 4. As shown in Tables 2, 3, and 4, the conversion of $CaCO_3$ to CH_4 is dependent on the presence of an equivalent amount of Ni and Al, which is needed in a 1: 2 mol ratio. To reduce the amount of Ni/Al alloy required for this conversion, an alternative approach was adopted, in which Al powder was also added. The initial mixture comprised 0.50 equivalents Ni/Al alloy and 1.0 equivalent of Al powder, resulting in an Al usage of approximately 2.0 equivalents. This mixture was subjected to a milling process, whereby $CaCO_3$ was converted to CH_4, with a conversion efficiency of 97% and H_2 generation efficiency of 62% (Table 5, Entry 1). Reducing the quantity of Ni/Al alloy powder from 0.50 equivalents to 0.10 equivalents, 0.05 equivalents and 0.01 equivalents resulted in a near-constant conversion efficiency of $CaCO_3$ to CH_4, as well as H_2 generation efficiency (Entries 2, 3, and 4). Furthermore, the conversion of $CaCO_3$ to CH_4 occurred with high efficiency, accompanied by H_2 generation (Entry 5), following the incorporation of 2.0 equivalents of Al. Despite increasing the Al molar equivalent to 4.6, the efficiencies of both $CaCO_3$ conversion to CH_4 and H_2 generation remained unchanged (Entry 6).

Subsequently, an investigation was conducted into the metal efficiencies of Ni, Fe, and Cr, the primary constituent metals of SUS. This study confirmed the conversion of $CaCO_3$ to CH_4 and the H_2 generation. The experiment was conducted using an 80 mL zirconia (ZrO_2) vessel and spherical balls (approximately 5 mm in diameter). The quantities of

Table 1
Reactivity of carbonates.

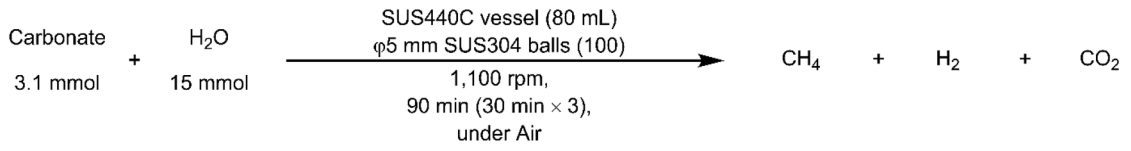

Entry	Carbonate	CH_4 Yield (%)[a)]	H_2 Yield (%)[a)]	CO_2 Yield (%)[a)]	H_2O Conversion (%)[a)]
1	Na_2CO_3	1	22	trace	22
2	K_2CO_3	trace	5	trace	5
3	$MgCO_3$	trace	trace	3	trace
4	$BaCO_3$	1	10	1	10
5	$CaCO_3$	1	2	trace	2
6	$FeCO_3$	8	70	10	73
7	$NiCO_3$	37	> 99	5	> 99
8[b)]	$NiCO_3$	60	> 99	2	> 99
9	$MnCO_3 \cdot nH_2O$	2	17	1[c)]	18
10	$CuCO_3 \cdot Cu(OH)_2$	2	trace	48	1
11	$ZnCO_3 \cdot Zn(OH)_2$	3	trace	53	1

a) Determined with GC-TCD
b) H_2O 10 mmol
c) CO was obtained in 5% Yield

Table 2
Effects of Ni species additives.

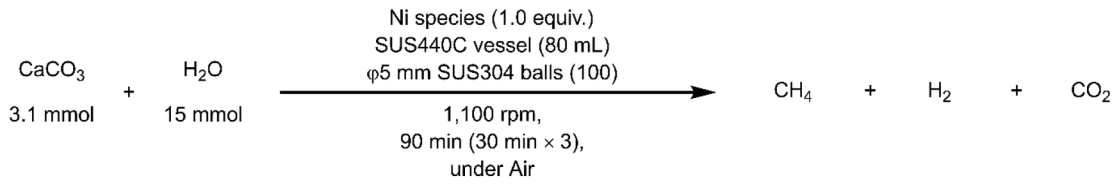

Entry	Ni species (1.0 equivalent)	CH_4 Yield (%)[a)]	H_2 Yield (%)[a)]	CO_2 Yield (%)[a)]	H_2O Conversion (%)[a)]
1	Ni/Al alloy	> 99	64	1	> 99
2	Ni	1	8	2	8
3	$Ni(OH)_2$	1	13	14	13
4	$Ni(OAc)_2 \cdot 4H_2O$	2	3	39	4
5	NiO	2	17	1	18
6	Raney Ni	1	10	trace	11

a) Determined with GC-TCD

Table 3
Effect of the effect of additives.

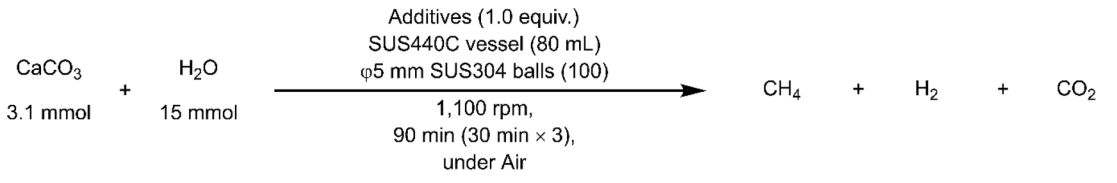

Entry	Additives (1.0 equivalent)	CH_4 Yield (%)[a)]	H_2 Yield (%)[a)]	CO_2 Yield (%)[a)]	H_2O Conversion (%)[a)]
1	Al	4	30	trace	32
2	Al_2O_3	7	64	trace	67
3	Ni + Al	18	71	trace	78
4	Ni + Al_2O_3	24	78	trace	88
5	Ni+ Al (2.0 equivalents)	> 99	39	trace	81

a) Determined with GC-TCD

Table 4
Effects the amount of Ni/Al alloy.

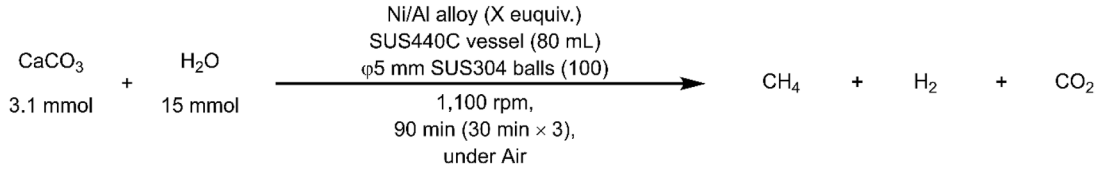

Entry	Ni/Al alloy (X equivalent)	CH_4 Yield (%)[a)]	H_2 Yield (%)[a)]	CO_2 Yield (%)[a)]	H_2O Conversion (%)[a)]
1	0.05	2	11	trace	12
2	0.10	4	17	trace	19
3	0.30	3	13	trace	14
4	0.50	7	36	trace	39

a) Determined with GC-TCD

H_2O and the number of balls were adjusted proportionally based on the vessel volume. This adjustment was necessary because the reactions observed with SUS304 balls, such as the conversion of H_2O to H_2 and the reduction of carbonates or CO_2 to CH_4, did not occur when ZrO_2 balls and the vessel were used in combination and milled [30]. In the experiment, $CaCO_3$ (3.1 mmol) and H_2O (270 μL, 15 mmol) were milled using ZrO_2 balls in a ZrO_2 vessel. This resulted in only 62% of the $CaCO_3$ being converted (decomposed) into CO_2 (Table 6, Entry 1), with negligible conversion of $CaCO_3$ to CH_4, as well as negligible H_2 generation. However, the addition of 2.0 equivalents of Al powder slightly improved the conversion efficiency of $CaCO_3$ to CH_4 (4%) and notably increased H_2 generation efficiency (31%) (Table 6, Entry 2). The incorporation of 1.0 equivalent of Ni/Al alloy into the mixture, as an alternative to Al powder alone, moderately enhanced the conversion of $CaCO_3$ to CH_4 (16%). Consequently, this led to a concomitant decrease in H_2 generation efficiency, which dropped to 15% (Entry 3). The addition of 1.0 equivalent of Ni powder and 2.0 equivalents of Al powder maintained a conversion efficiency of $CaCO_3$ to CH_4 at 16%, while increasing the H_2 generation efficiency to 28% (Entry 4). These results indicate that both mechanochemical energy and active metal surfaces are essential for the reaction. The absence of metallic components significantly reduces efficiency, highlighting the synergistic roles of mechanical activation and metal-mediated catalysis. These results demonstrate that Ni, Fe, and Cr in SUS304 balls and the SUS440C vessel contribute to both the

Table 5
Addition of supplementary Al powder in the presence of a catalytic quantity of Ni/Al alloy.

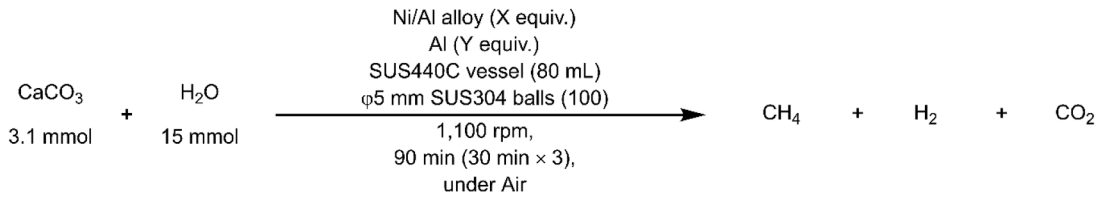

Entry	Ni/Al alloy (X equivalent)	Al (Y equivalent)	CH_4 Yield (%)[a)]	H_2 Yield (%)[a)]	CO_2 Yield (%)[a)]	H_2O Conversion (%)[a)]
1	0.50	1.0	97	62	1	> 99
2	0.10	1.8	86	54	1	89
3	0.05	1.9	88	64	1	> 99
4	0.01	1.98	75	48	1	79
5	-	2.0	84	63	1	97
6	-	4.6	87	69	1	> 99

a) Determined with GC-TCD

Table 6
Control experiments with ZrO_2 vessel and balls.

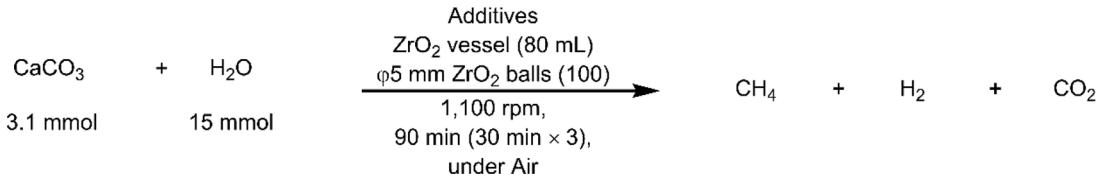

Entry	Additives (X equivalent)	CH_4 Yield (%)[a)]	H_2 Yield (%)[a)]	CO_2 Yield (%)[a)]	H_2O Conversion (%)[a)]
1	-	trace	trace	62	1
2	Al (2.0 equivalents)	4	31	28	35
3	Ni/Al (1.0 equivalent)	16	15	92	21
4	Ni (1.0 equivalent) + Al (2.0 equivalents)	16	28	49	35

a) Determined with GC-TCD

conversion of $CaCO_3$ to CH_4 and H_2 generation, with Ni being particularly significant. ICP analysis of the post-reaction mixture (see Supplementary Information) revealed significant amounts of Fe and Cr, likely originating from mechanical abrasion of the stainless-steel milling vessel and balls. In contrast, although Ni is present in stainless steel (e.g., ~8% in SUS304), the detected Ni likely originates predominantly from the Ni/Al alloy as is the case for Al. The elemental ratio (Fe > > Cr > Ni) is consistent with the composition of SUS304, indicating that Fe and Cr originate from mechanical abrasion rather than catalytic activity. These results suggest that the primary catalytic role is played by the Ni/Al alloy.

The effects of the Ni/Al alloy on other carbonates were investigated under the optimized conditions (Table 7). The conversion of $MnCO_3$, $CaCO_3$, and $CuCO_3$ to CH_4 was enhanced to near-quantitative yields, with efficient consumption of H_2O (Entries 5, 8, and 9). The conversion of $MgCO_3$, $FeCO_3$, and $NiCO_3$ to CH_4 was also significantly enhanced,

Table 7
Reactivity of carbonates in the presence of Ni/Al alloy.

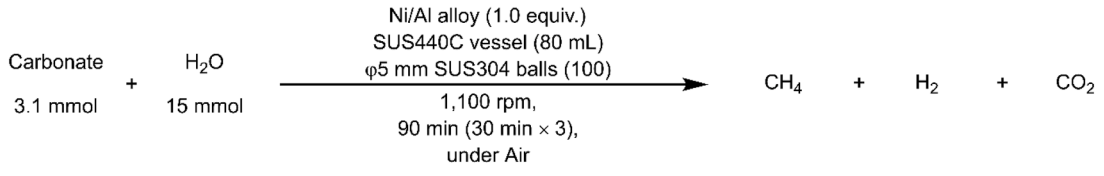

Entry	Carbonate	CH_4 Yield (%)[a)]	H_2 Yield (%)[a)]	CO_2 Yield (%)[a)]	H_2O Conversion (%)[a)]
1	Na_2CO_3	4	58	1	60
2	K_2CO_3	1	45	trace	46
3	$MgCO_3$	85	80	4	> 99
4	$BaCO_3$	12	77	1	82
5	$CaCO_3$	> 99	61	1	> 99
6	$FeCO_3$	76	79	1	> 99
7	$NiCO_3$	79	> 99	1	> 99
8	$MnCO_3 \cdot nH_2O$	> 99	57	1	> 99
9	$CuCO_3 \cdot Cu(OH)_2$	> 99	78	1	> 99
10	$ZnCO_3 \cdot Zn(OH)_2$	10	83	38	87

a) Determined with GC-TCD

accompanied by efficient consumption of H_2O (Entries 3, 6, and 7). In contrast, the conversion efficiencies of $BaCO_3$ and $ZnCO_3$ to CH_4 were approximately 10%, although H_2 generation was highly effective (Entries 4 and 10). In the cases of Na_2CO_3 and K_2CO_3, the conversion to CH_4 was only minimally affected by the addition of Ni/Al alloy, while the H_2 generation efficiency was noticeably enhanced (Entries 1 and 2). As the reaction progressed, a dynamic shift in the oxidation state of Ni in the Ni/Al alloy was observed, as evidenced by the Ni 2p XPS spectra (Fig. 1a–f). At the initial point in time (0 min), the predominant occurrence of Ni was observed in the metallic (zero valent) state, indicated by the primary peak at 852.8 eV. After 15 and 30 min (Fig. 1b and 1c), a distinct peak emerged at approximately 855.9 eV, thereby suggesting the formation of Ni (II) species. By 45 min (Fig. 1d), the Ni (II) peak at 856.5 eV became predominant, while the Ni (0) signal experienced a significant decline. Notably, at 60 min (Fig. 1e), the zero-valent Ni peak (852.2 eV) reappeared, while the Ni (II) signal diminished, suggesting that Ni is subsequently reduced back to its metallic form. At 90 min (Fig. 1f), only the Ni (0) peak (852.2 eV) was present, indicating complete regeneration of Ni in the zero-valent state. Reference samples of $NiCO_3$, $Ni(OH)_2$, and NiO (Fig. 1, g–i) provided further evidence that the Ni (II) species observed at 45 min correspond primarily to $NiCO_3$. As demonstrated in Table 1, $NiCO_3$ undergoes efficient methanation under these conditions, thereby explaining the subsequent reduction of the Ni (II) signal and restoration of Ni (0). Based on these observations, a plausible reaction pathway involves the formation of Ni (II) species such as $NiCO_3$, followed by their reduction to CH_4 with simultaneous regeneration of metallic Ni. Al plays a crucial role as an oxygen scavenger, preventing oxidation of Ni and sustaining catalytic activity.

These observations suggest that, under mechanochemical milling conditions, zero-valent Ni in the alloy may be partially oxidized to Ni (II) species [e.g., $NiCO_3$, $Ni(OH)_2$, or NiO], while the reduction of carbonates to CH_4 proceeds concurrently. As demonstrated in Table 1 (entries 7 and 8), given the relatively high reactivity of $NiCO_3$ towards methanation among various carbonates, it is conceivable that $CaCO_3$ may be converted to $NiCO_3$ and subsequently reduced to CH_4, with concomitant regeneration of metallic Ni. Aluminum, which has a high affinity for oxygen, is likely to act as an oxygen scavenger, thereby contributing to the suppression of Ni oxidation and the maintenance of catalytic activity.

Furthermore, XPS analysis of Al showed that the metallic Al peak at 71.8 eV, observed prior to the reaction, disappeared after the reaction, while a single peak at 74.1 eV was observed, consistent with the formation of Al_2O_3 (Fig. 2) [32,33]. Similarly, $CaCO_3$ (348.7 eV, 351.7 eV) appears to be converted to CaO (347.3 eV, 350.9 eV), as indicated by XPS analysis (Fig. 3) [34]. These findings suggest that metals other than Ni, such as Al, may act as oxygen scavengers, thereby suppressing the

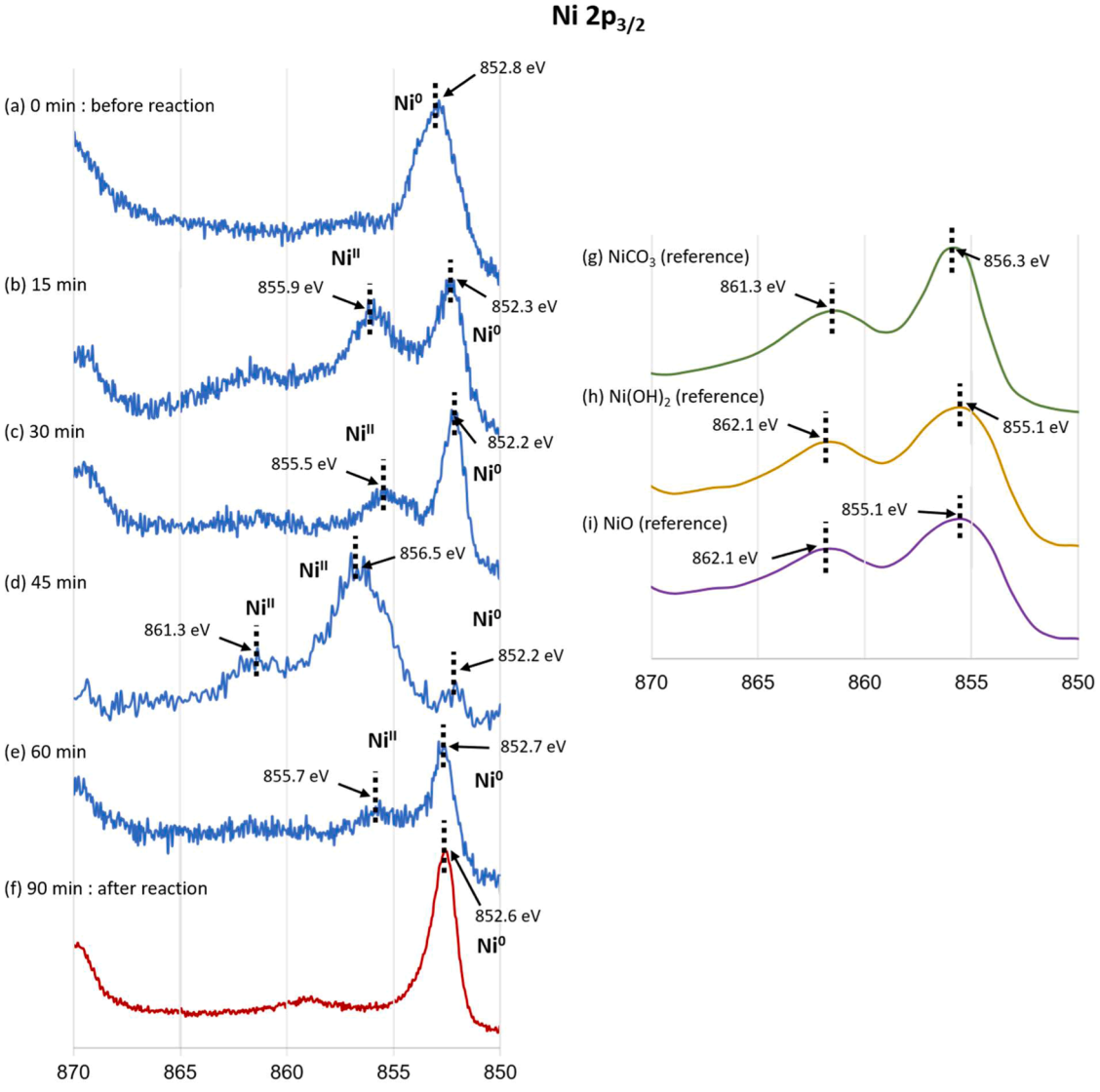

Fig. 1. Milling time-dependent XPS spectra (Ni 2p).

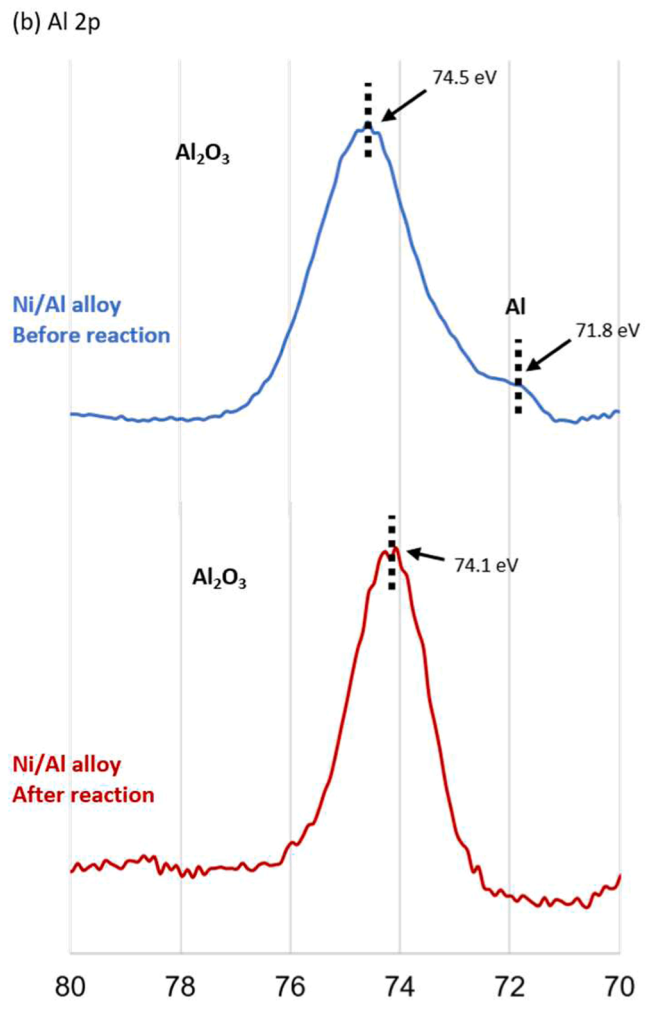

Fig. 2. Al 2p XPS spectra of Ni/Al alloy before and after the reaction.

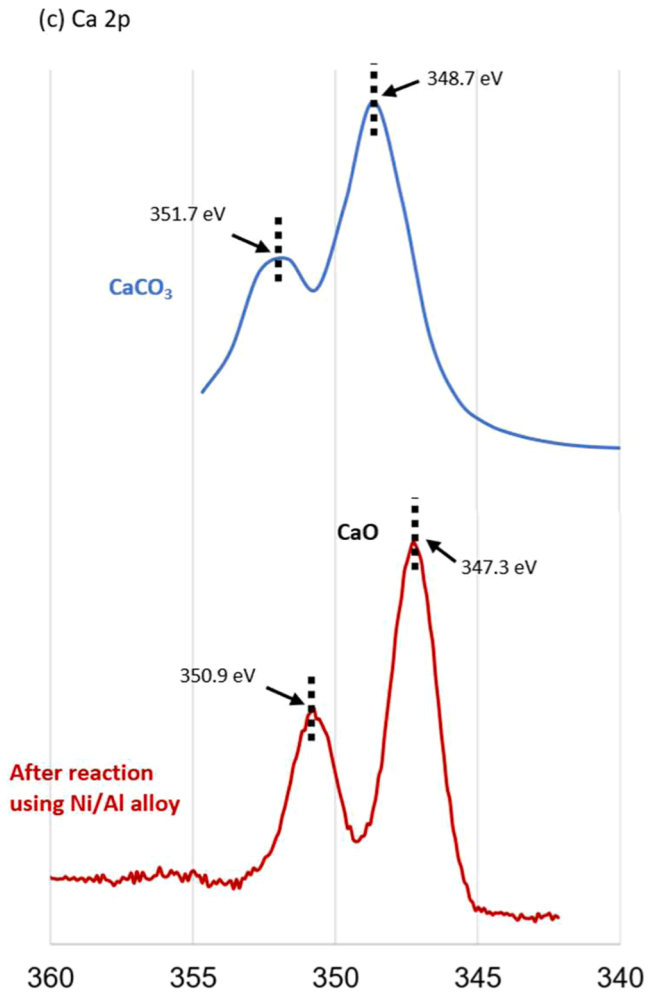

Fig. 3. Ca 2p XPS spectra of $CaCO_3$ before and after reaction.

oxidation of Ni. Consequently, these results suggest that zero-valent Ni species may retain their catalytic activity throughout the reaction, facilitating cation exchange from $CaCO_3$ to $NiCO_3$ and the subsequent methanation.

A powder X-ray diffraction (XRD) analysis of the reaction residue (see the Supplementary Information) indicates that the bulk structure of the Ni/Al alloy remains largely unchanged after the reaction. Furthermore, no distinct crystalline oxide phases were observed. These results suggest that the mechanochemical methanation proceeds primarily at the surface or at transient localized reaction sites, while the bulk structure of the materials remains largely preserved. This is consistent with the XPS results, which indicate dynamic surface transformations of Ni species during the reaction.

4. Conclusions

This study proposes a robust and innovative strategy for transforming carbonate salts into CH_4, using mechanochemical energy. The conversion was achieved via planetary ball milling in the presence of a Ni/Al alloy and H_2O, without H_2 or external heating. The process involved milling a mixture of carbonate, Ni/Al alloy, H_2O, and SUS304 balls within a SUS440C vessel. The proposed methodology avoids the use of complex and laborious operational procedures or stringent reaction conditions, such as precise temperature or pressure control, and maintenance of an oxygen-free environment. The novel approach presented in this study provides valuable insights into industrial applications and may contribute meaningfully to the development of a future carbon-neutral society.

Funding Information

This work was partially supported by a Grant-in-Aid from the Japan Society for the Promotion of Science (JSPS) KAKENHI (Grant Numbers 23K18190 and 25K21762) awarded to H.S., a Sasakawa Scientific Research Grant from the Japan Science Society (Grant Number 2025–3021) awarded to N.I., and the Japan Science and Technology Agency (JST) Support for Pioneering Research Initiated by the Next Generation (SPRING) Program (Grant Number JPMJSP2142) awarded to both N.I. and N.S.

CRediT authorship contribution statement

Naoya Ito: Writing – review & editing, Writing – original draft, Visualization, Methodology, Investigation, Funding acquisition, Formal analysis, Data curation. **Naoya Sakurada:** Writing – original draft, Validation, Investigation. **Tatsunori Iwamura:** Writing – review & editing, Writing – original draft, Methodology, Investigation, Formal analysis, Data curation. **Takashi Ikawa:** Writing – review & editing, Writing – original draft, Project administration, Data curation. **Hironao Sajiki:** Writing – review & editing, Writing – original draft, Supervision, Project administration, Methodology, Investigation, Funding acquisition, Formal analysis, Data curation, Conceptualization.

Declaration of competing interest

The authors declare that they have no known competing financial interests or personal relationships that could have appeared to influence the work reported in this paper.

Acknowledgements

This work was partially supported by a Grant-in-Aid from the Japan Society for the Promotion of Science (JSPS) KAKENHI (Grant Number 23K18190 and 25K21762) awarded to H.S, a Sasakawa Scientific Research Grant from the Japan Science Society (Number 2025–3021) awarded to N.I., and the JST Support for Pioneering Research Initiated by the Next Generation (SPRING) Program (Number JPMJSP2142) awarded to both N.I. and N.S. The authors thank Kawaken Fine Chemicals Co., Ltd. for kindly providing Ni/Al alloy. We also thank Editage (www.editage.jp) for English language editing.

Supplementary materials

Supplementary material associated with this article can be found, in the online version, at doi:10.1016/j.ceja.2026.101221.

Data availability

The data underlying this study are available in a published article and the Supporting Information.

References

[1] Conference of the parties serving as the meeting of the parties to the Paris agreement, report of the conference of the parties serving as the meeting of the parties to the Paris agreement on its third session, held in glasgow from 31 October to 13 November 2021. Addendum. Part two: action taken by the conference of the parties serving as the meeting of the parties to the Paris agreement at its third session (COP26 cover decision), 2021.
[2] S.A. Matlin, G. Mehta, S.E. Cornell, A. Krief, H. Hopf, Chemistry and pathways to net zero for sustainability, RSC Sustain. 1 (2023) 1704–1721, https://doi.org/10.1039/D3SU00125C.
[3] F. Gomollón-Bel, J. García-Martínez, Connecting chemical worlds for a sustainable future, Chem. Sci. 15 (2024) 5056–5060, https://doi.org/10.1039/D3SC06815C.
[4] S.C. Peter, Reduction of CO_2 to chemicals and fuels: a solution to global warming and energy crisis, ACS. Energy Lett. 3 (2018) 1557–1561, https://doi.org/10.1021/acsenergylett.8b00878.
[5] S.C. Peter, CO_2 hydrogenation to methanol: a contribution to carbon neutrality, ACS. Energy Lett. 10 (2025) 1139–1142, https://doi.org/10.1021/acsenergylett.5c00245.
[6] V. Kumaravel, J. Bartlett, S.C. Pillai, Photoelectrochemical conversion of carbon dioxide (CO_2) into fuels and value-added products, ACS. Energy Lett. 5 (2) (2020) 486–519, https://doi.org/10.1021/acsenergylett.9b02585.
[7] B. Chang, H. Pang, F. Raziq, S. Wang, K.-W. Huang, J. Ye, H. Zhang, Electrochemical reduction of carbon dioxide to multicarbon (C^{2+}) products: challenges and perspectives, Energy Env. Sci. 16 (2023) 4714–4758, https://doi.org/10.1039/D3EE00964E.
[8] X. Zhang, S.-X. Guo, K.A. Gandionco, A.M. Bond, J. Zhang, Electrocatalytic carbon dioxide reduction: from fundamental principles to catalyst design, Mater. Today Adv. 7 (2020) 100074, https://doi.org/10.1016/j.mtadv.2020.100074.
[9] R. Lu, Y. Liu, Z. Wang, Advances in the understanding of selective CO_2 reduction catalysis, EcoEnergy 2 (2024) 695–713, https://doi.org/10.1002/ece2.67.
[10] A. Beniwal, A. Bagaria, T. Chen, D. Bhalothia, Advancements in CO_2 conversion technologies: a comprehensive review on catalyst design strategies for high-performance CO_2 methanation, Sustain. Energy Fuels. 9 (2025) 2261–2286, https://doi.org/10.1039/D5SE00315F.
[11] S. Ullah, X. Yang, Z.U. Khan, S. Aziz, W. Haider, H. Ben, Relationship between catalyst structure and activity in CO_2 methanation of Ru-based catalysts: recent progress and future prospects, New. J. Chem. 49 (2025) 7097–7125, https://doi.org/10.1039/D5NJ00997E.
[12] N. Choudhary, K. Nabeela, N. Mate, S.M. Mobin, Recent advances in CO_2 hydrogenation to methane using single-atom catalysts, RSC Sustain. 2 (2024) 1179–1201, https://doi.org/10.1039/D4SU00020D.
[13] M. Tommasi, S.N. Degerli, G. Ramis, I. Rossetti, Advancements in CO_2 methanation: a comprehensive review of catalysis, reactor design and process optimization, Chem. Eng. Res. Des. 201 (2024) 457–482, https://doi.org/10.1016/j.cherd.2024.01.013.
[14] C. Faria, C. Rocha, C. Miguel, A. Rodrigues, L.M. Madeira, Process intensification concepts for CO_2 methanation: a review, Fuel 386 (2025) 134269, https://doi.org/10.1016/j.fuel.2024.134269.
[15] S. Ullah, Y. Gao, L. Dou, Y. Liu, T. Shao, Y. Yang, A.B. Murphy, Recent trends in plasma-assisted CO_2 methanation: a critical review of recent studies, Plasma Chem. Plasma Process. 43 (2023) 1335–1383, https://doi.org/10.1007/s11090-023-10417-9.
[16] J. Zhu, L. Lv, S. Zaman, X. Chen, Y. Dai, S. Chen, G. He, D. Wang, L. Mai, Advances and challenges in single-site catalysts towards electrochemical CO_2 methanation, Energy Env. Sci. 16 (2023) 4812–4833, https://doi.org/10.1039/D3EE01055F.
[17] N.D.M. Ridzuan, M.S. Shaharun, M.A. Anawar, I. Ud-Din, Ni-based catalyst for carbon dioxide methanation: a review on performance and progress, Catalysts 12 (5) (2022) 469, https://doi.org/10.3390/catal12050469.
[18] J. Kim, Ni catalysts for thermochemical CO_2 methanation: a review, Coatings 14 (10) (2024) 1322, https://doi.org/10.3390/coatings14101322.
[19] K. Liu, M.A. Nawaz, G. Liao, Progress and future challenges in designing high-performance Ni/CeO_2 catalysts for CO_2 methanation: a critical review, Carbon Neutraliz. 4 (1) (2025) e190, https://doi.org/10.1002/cnl2.190.
[20] C. Molinet-Chinaglia, S. Shafiq, P. Serp, Low temperature Sabatier CO_2 methanation, ChemCatChem 16 (24) (2024) e202401213, https://doi.org/10.1002/cctc.202401213.
[21] C. Padeste, A. Reller, H.R. Oswald, The influence of transition metals on the thermal decomposition of calcium carbonate in hydrogen, Mater. Res. Bull. 25 (10) (1990) 1299–1305, https://doi.org/10.1016/0025-5408(90)90088-J.
[22] A. Tsuneto, A. Kudo, N. Saito, T. Sakata, Hydrogenation of solid state carbonates, Chem. Lett. 21 (5) (1992) 831–834, https://doi.org/10.1246/cl.1992.831.
[23] N. Yoshida, T. Hattori, E. Komai, T. Wada, Methane formation by metal-catalyzed hydrogenation of solid calcium carbonate, Catal. Lett. 58 (1999) 119–122, https://doi.org/10.1023/A:1019017615013.
[24] C. Mesters, N. Rahimi, D. van der Sloot, J. Rhyne, F. Cassiola, Direct reduction of magnesium carbonate to methane, ACS. Sustain. Chem. Eng. 9 (2021) 10977–10989, https://doi.org/10.1021/acssuschemeng.1c01439.
[25] T. Shen, J. Wu, Q. Liu, Z. Liu, Hydrogenation of $CaCO_3$ for methane by a liquid organic hydrogen carrier, Ind. Eng. Chem. Res. 62 (2023) 10721–10728, https://doi.org/10.1021/acs.iecr.3c01314.
[26] S. Shi, Y. Zhang, Y. Pan, X. Liu, F. Zhang, H. Yang, Q. Liu, Z. Liu, Hydrogenation of $CaCO_3$ to CH_4 catalyzed by $NiCO_3$, Chem. Eng. J. 485 (2024) 150012, https://doi.org/10.1016/j.cej.2024.150012.
[27] S. Shi, J. Yu, Y. Pan, Y. Zhang, H. Yang, T. Shen, Q. Liu, Z. Liu, Hydrogenation of calcium carbonate to carbon monoxide and methane, Fuel 354 (2023) 129385, https://doi.org/10.1016/j.fuel.2023.129385.
[28] Y. Sawama, M. Niikawa, Y. Yabe, R. Goto, T. Kawajiri, T. Marumoto, T. Takahashi, M. Itoh, Y. Sasai, Y. Yamauchi, S. Kondo, M. Kuzuya, H. Sajiki, Stainless-steel-mediated quantitative hydrogen generation from water under ball milling conditions, ACS. Sustain. Chem. Eng. 3 (2015) 683–689, https://doi.org/10.1021/sc5008434.
[29] Y. Sawama, N. Yasukawa, K. Ban, R. Goto, M. Niikawa, Y. Monguchi, M. Itoh, H. Sajiki, Stainless steel-mediated hydrogen generation from alkanes and diethyl ether and its application for arene reduction, Org. Lett. 20 (2018) 2892–2896, https://doi.org/10.1021/acs.orglett.8b00931.
[30] Y. Sawama, T. Kawajiri, M. Niikawa, R. Goto, Y. Yabe, T. Takahashi, T. Marumoto, M. Itoh, Y. Kimura, Y. Monguchi, S. Kondo, H. Sajiki, Stainless-steel ball-milling method for hydro-/deutero-genation using H_2O/D_2O as a hydrogen/deuterium source, ChemSusChem 8 (2015) 3773–3776, https://doi.org/10.1002/cssc.201501019.
[31] Y. Sawama, M. Niikawa, K. Ban, K. Park, S. Aibara, M. Itoh, H. Sajiki, Quantitative mechanochemical methanation of CO_2 with H_2O in a stainless steel ball mill, Bull. Chem. Soc. Jpn. 93 (2020) 1074–1078, https://doi.org/10.1246/bcsj.20200105.
[32] G. Ma, Y. Zhao, H. Cui, X. Song, M. Wang, K. Lee, X. Gao, Q. Song, C. Wang, Addition Al and/or Ti induced modifications of microstructures, mechanical properties, and corrosion properties in CoCrFeNi high-entropy alloy coatings, Acta Met. Sin. Engl. Lett. 34 (2021) 1087–1102, https://doi.org/10.1007/s40195-021-01219-z.
[33] S.E. Collins, D.L. Chiavassa, A.L. Bonivardi, M.A. Baltanás, Hydrogen spillover in Ga_2O_3–Pd/SiO_2 catalysts for methanol synthesis from CO_2/H_2, Catal. Lett. 103 (2005) 83–88, https://doi.org/10.1007/s10562-005-6507-5.
[34] J. Liu, M. Liu, S. Chen, B. Wang, J. Chen, D.-P. Yang, S. Zhang, W. Du, Conversion of Au (III)-polluted waste eggshell into functional CaO/Au nanocatalyst for biodiesel production, Green Energy Env. 7 (2) (2022) 352–359, https://doi.org/10.1016/j.gee.2020.07.019.